Numerical Simulation and Experimental Research of Multi-stage Roots Vacuum Pump

Kai Ma, Hongye Qiu, Dantong Li, Chongzhou Sun, Lantian Ji, Bingqi Wang, Weifeng Wu, Zhilong He
School of Energy and Power Engineering, Xi'an Jiaotong University, Xi'an 710049, China;
Email: monkey8023@stu.xjtu.edu.cn

Abstract. Multi-stage roots pump is generally used as vacuum pump, which have medium tolerance and high gas flow. Multi-stage roots vacuum pump (MSRVP) is often used in the semiconductor and photovoltaic industries. The rotor of the MSRVP is a straight-blade rotor, so the theoretical internal pressure ratio of MSRVP is 0, and the pressure distribution in the cavity is established by leakage. One-dimensional working process simulation is difficult to predict its performance and internal flow. It is necessary to intuitively understand the mechanism of internal flow heat transfer in multi-stage roots through experiments and three-dimensional simulation. The MSRVP studied in this paper is six-stage rotor with two-lobes. A three-dimensional internal flow field model of a MSRVP is established, and a performance test bench is built to measure its performance. The experimental results are in good agreement with the three-dimensional simulation results. The simulation results reflect the fluid flow inside the MSRVP, and the pressure established by the internal leakage can be obtained more clearly.

1. Introduction

Dry vacuum pumps continue to improve with the rapid development of high-tech semiconductors. As one of the MSRVP, it is widely used in industries such as semiconductors, scientific instruments, and biological products. MSRVP has the advantages of wide pumping speed range, stable operation, low vibration and noise, etc. Compared with single-stage vacuum pumps, MSRVP differ in that the internal structure is 3-5 stages of rotors connected in series on the rotor shaft. The rotors of each stage are connected through inter-stage channels[1,2]. The connected chamber can be realized by radial bypass or axial connection. The rotors of MSRVP mainly have two-lobes, three-lobes and five-lobes rotor forms, and the diameter or phase angle of the rotor can vary[3,4]. In addition, the profile of the Roots vacuum pump rotor can be symmetrical or asymmetrical[5].

The mathematical model of the MSRVP can predict the working characteristics of the vacuum pump when the operating or structure parameters is changed. It's necessary to the research the performance of the MSRVP. There are mainly two ways to study the MSRVP[6-9]. One is to establish a reasonable Roots vacuum pump leakage model through theory or experiment, so as to establish a reasonable pressure distribution and obtain its performance. Laurent-Charles et. al[10] used semi-empirical Knudsen-Dong law to calculate the conductance of each clearances to peridiction the internal leaks of dry Roots vacuum pump. S. R. In et. al [11]estimated the different leak channels as a rectangular channel with a circular profile of short duct length, and analysed the impact of different structural and operating parameters on performance. A.A.Raykov et. al [12] developed the conductance calculation procedure of radial channels of Roots vacuum pump. A. Isaev et. al [13] proposed the method based on energy balance of thermodynamic system to calculate the characteristics of Roots Pump. In addition to theory, a more commonly used tool is to use CFD to calculate the performance of Roots pumps[14-15]. Chiu-Fan Hsieh et. al [16] analysed the flow characteristics of a gerotor type vacuum pump connected in serial and parallel. Y B Li et. al [17] used unstructured grids to calculate the effects of pressure angle on the performance of Roots Pump. Shu-Kai Sun et. al [18] established a 3D model and compared the difference between the 2D and 3D models. The result prove the accuracy of the 2D model in flow and pressure distribution. There are few numerical studies on MSRVP, and numerical models are often limited to a single machine. Furthermore, no detailed study of the flow field inside the MSRVP.

In order to better study the internal pressure building process of the pump, this paper established a three-dimensional numerical model of the MSRVP by structured grids, and simulated the performance of the MSRVP by using CFD technology. The flow characteristics of the internal fluid inside the pump are analyzed, and the pressure distributions are obtained. The simulation and experimental results are in good agreement. And the model can be used for MSRVP with different stages, different lobes, variable diameters and variable phase angles.

2. Geometric Structure

The multi-stage Roots rotor studied in this paper is a six-stage Roots rotor, and its profile is shown in Figure 1. The rotor has a six-stage structure, and the rotor profile of each stage is the same. The profile of the Roots rotor is composed of circular arcs and conjugate curves of the circular arcs. Due to the compact structure and the need for a larger suction flow area, the first stage rotor is located in the second position. The structure of the MSRVP rotor is shown in Figure 2. The rotors are 2nd, 1st, 3rd, 4th, 5th, and 6th stage rotors from left to right.

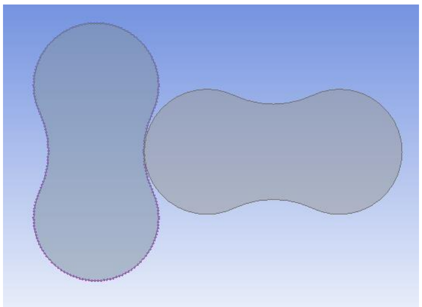

Figure 1. The rotor profile of the multi-stage Roots vacuum pump

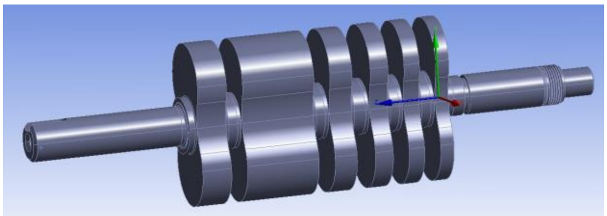

Figure 2. The structure of multi-stage Roots rotor

The gap of the PZ refers to the positive direction of the Z direction, which is the gap between the rotor and the suction side. The MZ refers to the gap in the oppositive direction of the Z direction. The specific structural parameters of the multistage Roots rotor are shown in Table 1.

Table 1. The parameters of the multi-stage Roots rotor

Stage	Rotor Length[mm]	Gap of the PZ[mm]	Gap of the MZ[mm]	Cylinder Diameter[mm]
1	31.8	0.05	0.05	70
2	12.8	0.05	0.05	70
3	9.8	0.05	0.05	70
4	7.85	0.05	0.05	70
5	6.85	0.05	0.05	70
6	5.9	0.05	0.05	70

Table 1 show that the rotors of each stage have the same gap of MZ and PZ, and the center distance between the two rotors is 48mm.

There are two connection methods between the roots of each stage. The connection methods of the different stage are shown in Figure 3. One is that the gas connection path is in the radial direction of the rotor. The path of each stage is air intake on the upper side and exhaust on the lower side. The intake and exhaust passages are connected outside the cylinder. The other is that the rotors of different stages are connected axially, and the connection path is located in the housing between the rotor stages. After the exhaust gas from the lower side enters the upper side of the next stage through the interstage casing, the connection between the stages is realized. The MSRVP studied in this paper adopts the method of radial connection.

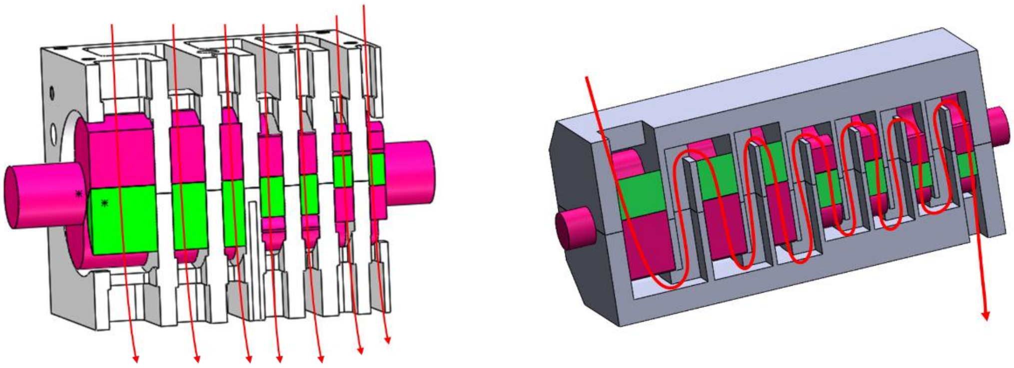

(a) The gas radially connected between different stage rotors

(b) The gas axially connected between different stage rotors

Figure 3. The method of gas connection between different rotors

3. Mesh Generation and Simulation Setup

There are multiple working chambers in the MSRVP, and the working process is very complicated. In order to simulate the working process of MSRVP, the fluid model is divided into two parts. One is static fluid domain and the other is rotating fluid domain. The static fluid domain of the MSRVP is shown in Fig.4. Among them, the static flow domain includes the suction flow domain, the exhaust flow domain and five inter-stage connected flow domains. The rotating flow domain is divided into 1 to 6 lobes of rotating flow domain. In the calculation process, connect all the parts and exchange data information through the interface. The control volume domain of the MSRVP is shown in Fig.5.

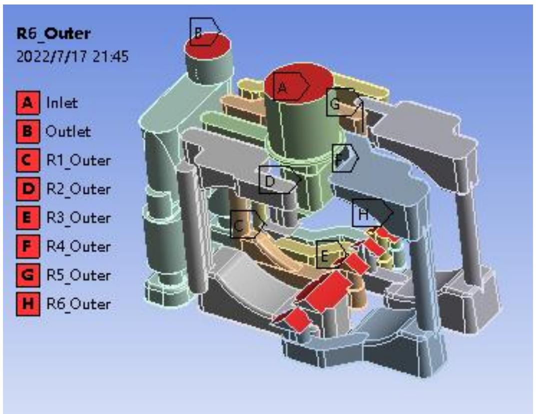

Figure 4. The static fluid domain of the MSRVP

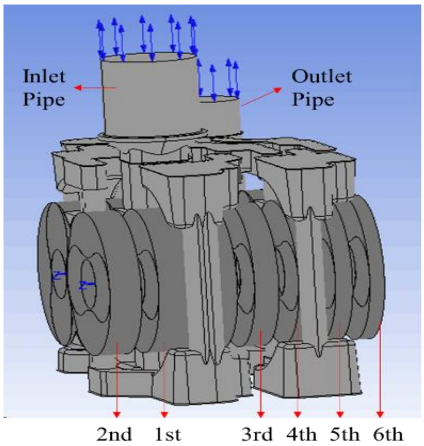

Figure 5. The control volume fluid domain of the MSRVP

The mesh of static fluid domain of the MSRVP is generated by ANSYS-Mesh, and all the static fluid mesh is generated by the same method. For the inlet, outlet and inter-stage connected domain have complex shape, so the mesh size function of Proximity and Curvature is used. For the rotating fluid domain, the mesh is generated by the software TwinMesh. The 2D rotating grids is generated with 20 radial nodes and 61 Interface nodes. The rotating grids can meets the quality requirements through node settings. The meshing of the 2D seciton is shown in Figure 6.

Due to the different lengths of the rotors of different stages, the number of mesh layers in the axial direction is different. The number of axial grid layers of the multi-stage Roots rotor is proportional to the length of the rotor, and the grid length is less than 1mm. The rotating fluid grids of the chamber volume is shown in Figure 6.

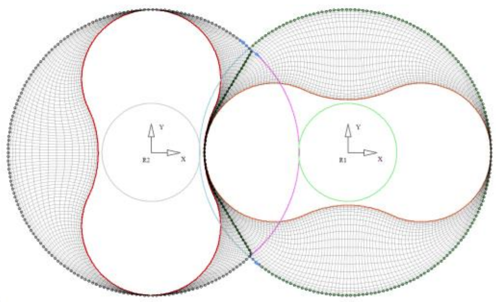

Figure 6. The meshing of the 2D section

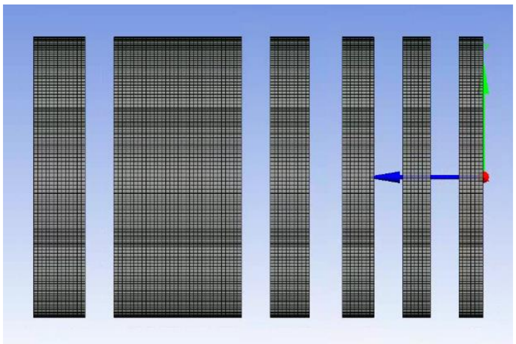

Figure 7. The rotating fluid grids of the chamber volume

The internal fluid in the chamber should comply with the laws of conservation of physics, including the law of conservation of mass, the law of conservation of momentum and the law of conservation of energy. The system also needs to comply with additional turbulent transport equations. For the numerical simulation of rotating machinery, the shear pressure transmission (SST) k-ω model combines the far-field k-ε model and the near-wall k-ω model the SST (Shear Stress Transport) model, which can obtain more accurate results.

$$\frac{\partial}{\partial t}(\rho k) + \frac{\partial}{\partial x_i}(\rho k u_i) = \frac{\partial}{\partial x_j}\left(\Gamma_k \frac{\partial \omega}{\partial x_j}\right) + G_\omega - Y_\omega + D_\omega + S_\omega \tag{1}$$

$$\frac{\partial}{\partial t}(\rho\omega) + \frac{\partial}{\partial x_i}(\rho\omega u_i) = \frac{\partial}{\partial x_j}\left(\Gamma_\omega \frac{\partial k}{\partial x_j}\right) + G_k - Y_k + S_k \tag{2}$$

The boundary conditions of the suction and exhaust ports is set to opening conditon. The inlet pressure is set to 0.01bar, and the temperature is 293.15K. The outlet pressure is set to 1.0bar, and the return temperature is 293.15K. The surface temperature of the pump body is an isothermal boundary, and the temperature is 60°C.

Since the dynamic mesh of the rotation domain in this paper is generated by TwinMesh, the time step is related to the angular step of rotation, and this mesh is generated with 2° angular step.

4. Case Studies

This paper use a six-stage MSRVP to build a vacuum pump performance test bench. The MSRVP performance test bench system diagram is shown in Figure 8. The system is composed of MSRVP, mass flow meter, vacuum test chamber, and vacuum gauge.

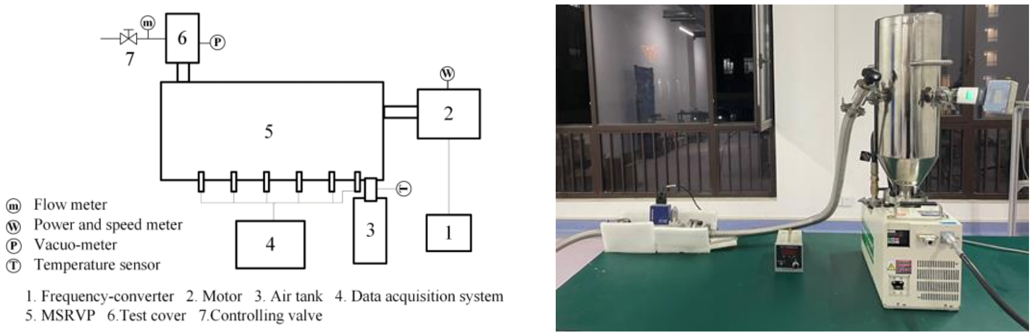

Figure 8. The MSRVP performance test bench

In this experiment, by adjusting the opening of the valve and the reading of the vacuum gauge, the pumping speed curve of the MSRVP at the rated speed is measured. The pumping speed curve of the MSRVP is shown in Figure 9. The pumping speed of the MSRVP rises to the maximum value first, and the maximum suction speed is maintained at 100-1000Pa at about 500 liters per minute. At 50000-100000Pa, the pumping speed is about 170 liters per minute.

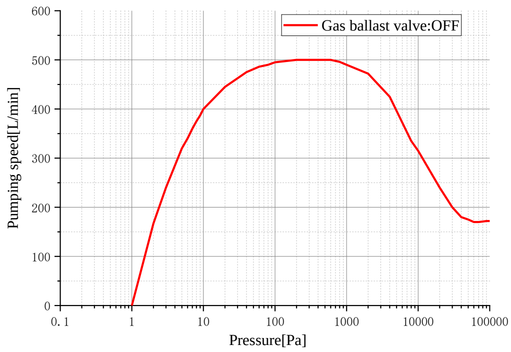

Figure 9. The S-P curves

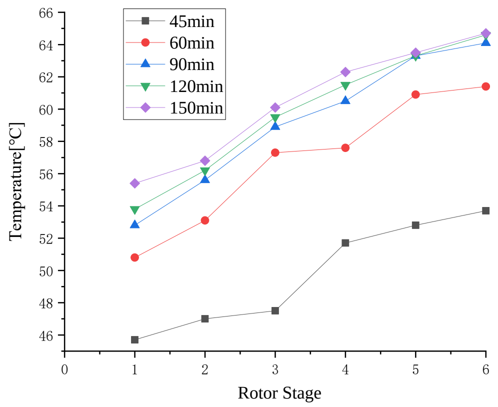

Figure 10. The relationship between the shell surface temperature and time

Arrange temperature measuring points on the surface of each chamber of the MSRVP, and monitor the change of body surface temperature with time. After the MSRVP runs for 30 minutes, record the temperature of the measuring point at intervals of 15 minutes. After running for 60 minutes, record the temperature of the measuring point at intervals of 30 minutes. The change curve of the surface temperature of the body with time is shown in Figure 10.

Within 90 minutes of running time, there is a large temperature rise on the surface of the chamber. From 45 minutes to 60 minutes, the temperature rise is about 7°C, and from 60 minutes to 90 minutes, the temperature rise is about 3°C. After subsequent operation, the temperature rise of the surface temperature of the chamber changes little. The average surface temperature of the cavity is about 60°C. Under different conditions, measure the temperature of the surface of each cavity, and the average value of the surface temperature measurement points is the temperature of the chamber in the numerical simulation.

5. Results

The MSRVP s adopts the method of radial connection. It’s hard to punch holes to measure icacity pressure. In order to verify the accuracy of the three-dimensional flow field model of the MSRVP, this paper compares the experimental and simulated values of the pumping speed. As shown in Figure 11, the figure shows the difference between simulated value and the experimental value at rated speed and the different inlet pressures. The error between the simulated value and the experimental value is shown in Table 2.

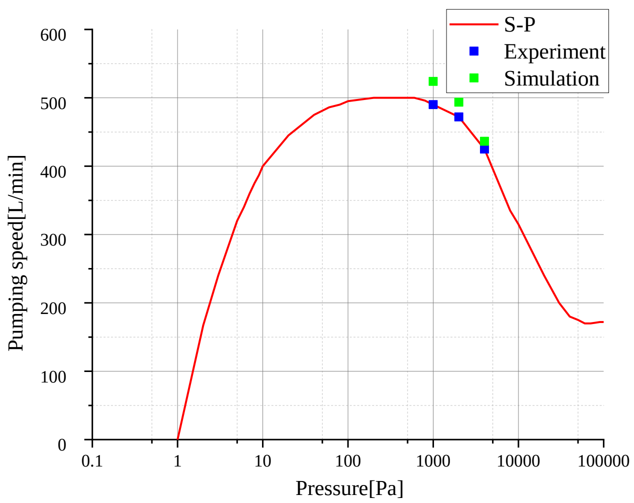

Figure 11. Comparison of simulated data and experimental data

Table 2. The comparison results of the MSRVP simulated values and experimental values

Suction Pressure[Pa]	Experimental Pumping Speed [L/min]	Simulated Pumping Speed [L/min]	Error [%]	Experimental Electric Power [W]	Simulated Shaft Power [W]
1000	490.8	523.9	6.74	342	231.71
2000	472.6	493.5	4.42	354	243.42
3000	425.7	436.3	2.49	365	255.64

There are two main reasons for the difference between the simulation and the experiment. One is that the inlet pressure is low, and the flow state of the fluid is molecular-viscous flow, which leads to inaccurate CFD calculations. Another reason is that the temperature on the surface of the chamber adopts an isothermal wall, and the simulation uses an average temperature of 60°C, rather than the actual wall temperature, which basically follows a linear distribution ranging from 56-64°C.

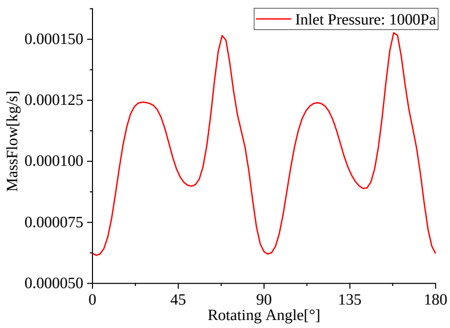

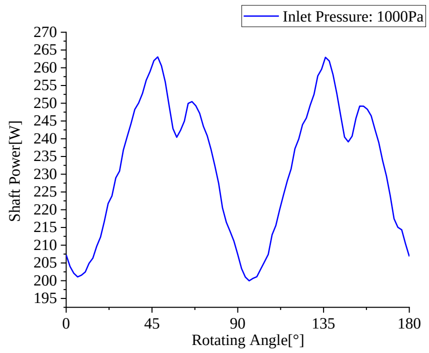

Figure 12. The mass flow rate changes with rotating angle

Figure 13. The shaft power changes with rotating angle

The inlet mass flow rate and rotor shaft power when the inlet pressure is 1000Pa are shown in Figure 12 and Figure 13. Due to the asymmetrical rotation of the rotor, the mass flow at the inlet has asymmetrical periodic fluctuations. There are two peaks in the mass flow of the inlet, the peaks are 0.000124 kg/s and 0.0001515 kg/s respectively. The shaft power is only generated by the gas acting on the rotor, excluding mechanical and frictional losses. However, the electric power includes the power of the transformer, the power of the cooling fan and the input power of the MSRVP. This is the difference between the electrical power and the shaft power. The difference between the experimental electric power and the simulated shaft power is close to a fixed value, which is 110W. The pressure distribution of the flow field in the MSRVP is calculated by CFD software. The MSRVP can be analyzed according to the axial pressure distribution of the rotor. The rotor of the MSRVP is a two-lobes rotor, and the rotor rotation period is 180°. At intervals of 30°, analyze the variation of intracavity pressure within a cycle. The pressure range in the MSRVP chamber is from 1000Pa to 100000Pa. In order to clearly reflect the pressure range of different stages of the chamber, the logarithmic coordinate system legend is used.

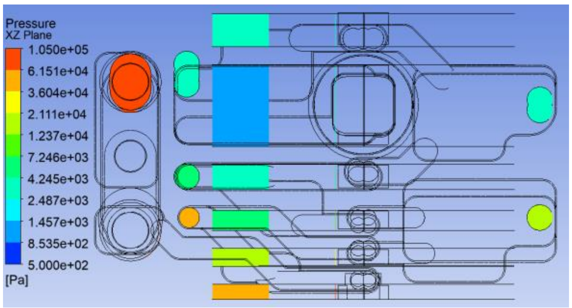

(a) Angle=30°

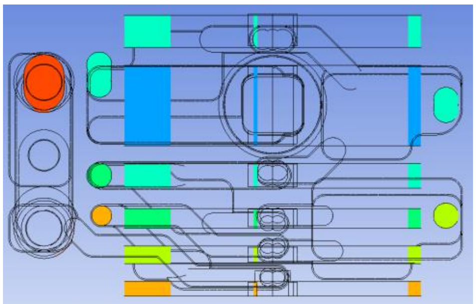

(b) Angle=60°

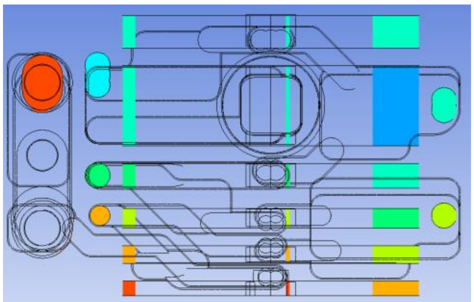

(c) Angle=90°

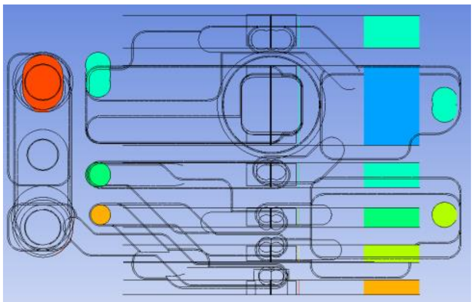

(d) Angle=120°

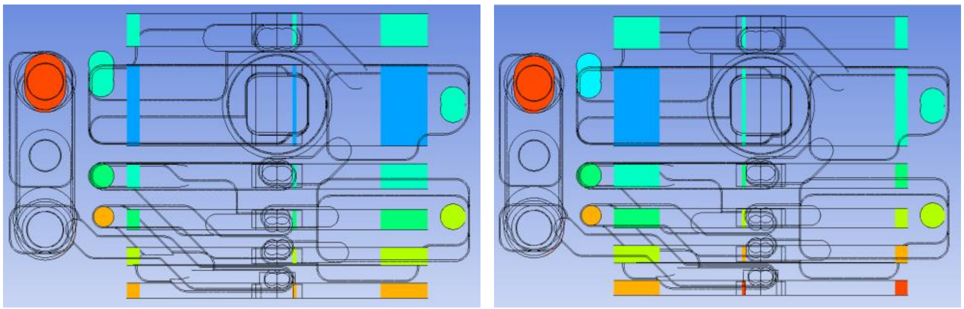

(e) Angle=150°　　　　(f) Angle=180°

Figure 14. The pressure distribution in the MSRVP

Figure 14 reflects the change of pressure in the cavity and the connecting chamber in a period. The pressure in the chamber shows an upward trend from the first stage to the sixth stage . Since the rotor profiles of different stages are the same and the phase angles are the same, the suction and exhaust of the six stages are carried out at the same time. And the pressure fluctuation in the connected chamber is affected by the exhaust pressure of the previous stage, the suction pressure of the subsequent stage and its length and shape. The monitoring points are set at the beginning and end of the connecting cavity, and the pressure fluctuations also change periodically.

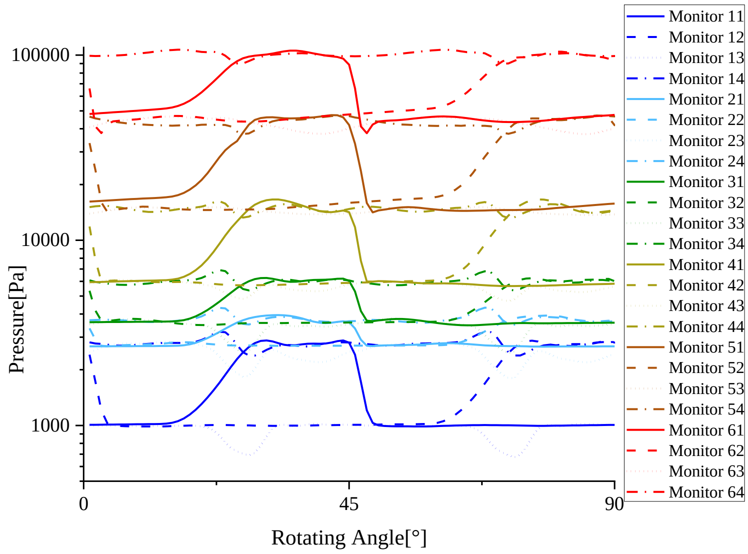

Figure 15. The pressure changes of the six-stage chamber

The pressure change in the chamber of the six-stage Roots vacuum pump is shown in Figure 15. For the change in the chamber of each stage, the change rule is the same as that of the single-stage Roots pump, which changes periodically, and only the inlet and outlet pressures are different. This article does not analyse the pressure change of a single stage, but mainly analyses the axial pressure change. The pressure range of the 1st chamber of the MSRVP is about 1000-2800Pa, 2nd chamber of 2800-3600Pa, and 3rd chamber of 3600-5800Pa. The pressure difference range of the first three stages is about 2000pa, and from the fourth stage, the pressure difference between the two stages becomes larger. The suction and exhaust pressure difference is about 10000Pa at the fourth stage, about 30000Pa at the fifth stage, and about 55000Pa at the sixth stage. The relative value of the pressure fluctuation in the connected chamber gradually decreases with the increase of the number of stages.

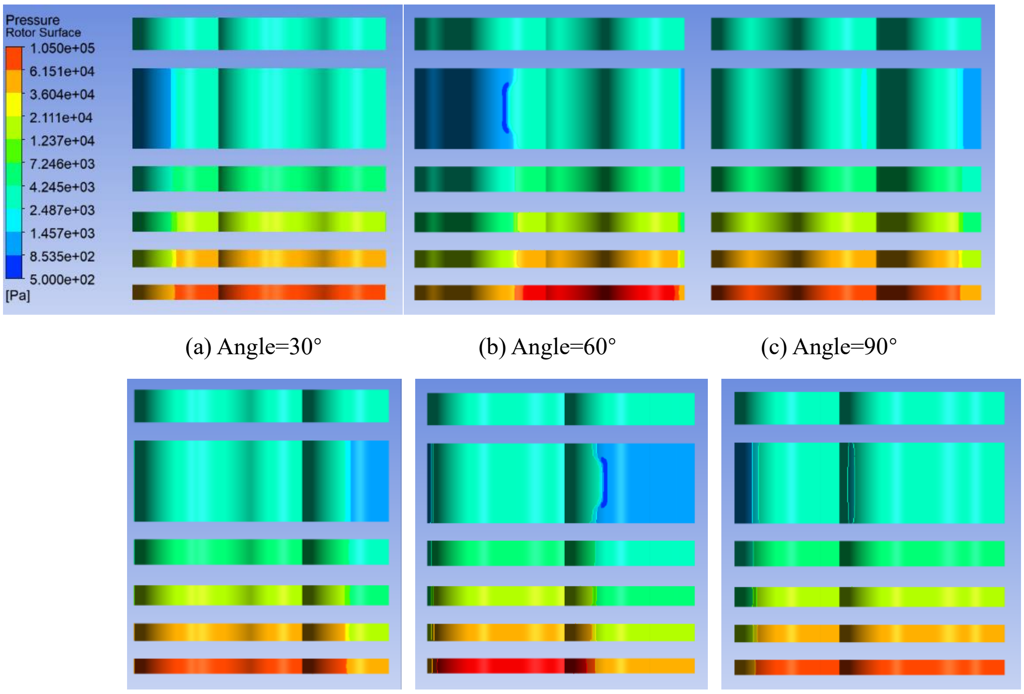

(a) Angle=30° (b) Angle=60° (c) Angle=90°

(d) Angle=120° (e) Angle=150° (f) Angle=180°

Figure 16. The pressure distribution on the rotor surface

Figure 16 reflects the distribution of the pressure on the rotor surface. The boundary line of different colors on the surface of the rotor is the leakage line when the gap between the rotor and the casing is the smallest. Outside the area affected by the non-inlet and non-exhaust ports, the boundary line is a straight line.The boundary line is affected by the intake and exhaust fluctuations, and the shape of the boundary is similar to that of the intake and exhaust ports.

6. Conclusions

This paper establish a three-dimensional numerical model of the MSRVP, built a performance test bench and analyse the internal fluid field of the pump. The conclusions are as follows.

1) The internal flow field model of MSRVP is established and the performance test bench was built to test the pumping speed and surface temperature. The simulated and experimental values are in good agreement.So the model can be used for MSRVP with different stages, different lobes, variable diameters and variable phase angles;
2) The axial pressure of MSRVP increases according to the number of stages, showing a trend of slow first and then fast. The relative value of the pressure fluctuation in the connected chamber gradually decreases with the increase of the number of stages.

References

[1] Sun, S. K., Jia, X. H., Xing, L. F., & Peng, X. Y. (2018). Numerical study and experimental validation of a Roots blower with backflow design. Engineering Applications of Computational Fluid Mechanics, 12(1), 282-292.

[2] Hsieh, C. F., & Deng, Y. C. (2015). A design method for improving the flow characteristics of a multistage Roots pumps. Vacuum, 121, 217-222.

[3] Hsieh, C. F., & Zhou, Q. J. (2015). Fluid analysis of cylindrical and screw type Roots vacuum pumps. Vacuum, 121, 274-282.

[4] Singh, G., Sun, S., Kovacevic, A., Li, Q., & Bruecker, C. (2019). Transient flow analysis in a Roots blower: Experimental and numerical investigations. Mechanical Systems and Signal Processing, 134, 106305.

[5] Wang, J., Yang, S., Sha, R., Li, H., & Xu, C. (2020). Geometric Design and Analysis of Novel Asymmetrical Rotors for Roots Vacuum Pumps. Journal of Mechanical Design, 142(6).

[6] Wu, Y. R., & Tran, V. T. (2018). Generation method for a novel Roots rotor profile to improve performance of dry multi-stage vacuum pumps. mechanism and machine Theory, 128, 475-491.

[7] Joshi, A. M., Blekhman, D. I., Felske, J. D., Lordi, J. A., & Mollendorf, J. C. (2004). Clearance analysis and leakage flow CFD model of a two-lobe multi-recompression heater. International Journal of Rotating Machinery, 2006.

[8] Guo, Q., Luo, K., Li, D., Huang, C., & Qin, K. (2021). Effect of Operating Conditions on the Performance of Gas–Liquid Mixture Roots Pumps. Energies, 14(17), 5361.

[9] Li, Y., Guo, D., Fan, Z., & Du, J. (2020). Effects of different blade numbers on radial exciting force of Lobe pump Rotor. International Journal of Fluid Machinery and Systems, 13(2), 281-291.

[10] Valdès, L. C., Barthod, B., & Le Perron, Y. (1999). Accurate prediction of internal leaks in stationary dry Roots vacuum pumps. Vacuum, 52(4), 451-459.

[11] In, S. R., & Kang, S. P. (2015). Analysis of Pumping Characteristics of a Multistage Roots Pump. Applied Science and Convergence Technology, 24(1), 9-15.

[12] Raykov, A. A., Tyurin, A. V., Burmistrov, A. V., Salikeev, S. I., Bronstein, M. D., & Fomina, M. G. (2019, August). Calculation of backward flow in channels with moving walls in oil free non-contact vacuum pumps. In AIP Conference Proceedings (Vol. 2141, No. 1, p. 030024). AIP Publishing LLC.

[13] Isaev, A., Raykov, A., Burmistrov, A., Salikeev, S., & Kapustin, E. (2020, November). Development of calculation method based on energy balance of thermodynamic system of variable mass body for roots pumps. In AIP Conference Proceedings (Vol. 2285, No. 1, p. 030042). AIP Publishing LLC.

[14] Li, Y. B., Du, J., & Guo, D. S. (2019). Numerical research on viscous oil flow characteristics inside the rotor cavity of rotary lobe pump. Journal of the Brazilian Society of Mechanical Sciences and Engineering, 41, 1-11.

[15] Xing, W., Zhang, F., Zhao, F., Song, J., Zhu, X., & Tang, X. (2022). Influence of Different Reflux Groove Structures on the Flow Characteristics of the Roots Pump. Machines, 10(11), 1087.

[16] Hsieh, C. F., Johar, T., & Li, Y. T. (2022). Flow characteristics of gerotor vacuum pumps with multistage designs. Vacuum, 196, 110787.

[17] Li, Y. B., Jia, K., Meng, Q. W., Shen, H., & Sang, X. H. (2013, December). Flow simulation of the effects of pressure angle to lobe pump rotor meshing characteristics. In IOP Conference Series: Materials Science and Engineering (Vol. 52, No. 3, p. 032022). IOP Publishing.

[18] Sun, S. K., Zhao, B., Jia, X. H., & Peng, X. Y. (2017). Three-dimensional numerical simulation and experimental validation of flows in working chambers and inlet/outlet pockets of Roots pump. Vacuum, 137, 195-204.